

1 **Altered Decorin Leads to Disrupted Endothelial Cell Function: A Possible**
2 **Mechanism in the Pathogenesis of Fetal Growth Restriction?**

3
4 Chui A ¹, Murthi P ^{2,3}, Gunatillake T ^{1,3}, Brennecke S.P ^{2,3}, Ignjatovic V ^{4,5,6}, Monagle P.T
5 ^{4,5,6}, Whitelock J.M ⁷, and Said J.M¹

6
7 ¹NorthWest Academic Centre, The University of Melbourne and Sunshine Hospital, St
8 Albans 3021, Australia. ²Department of Perinatal Medicine, Pregnancy Research
9 Centre, The Royal Women's Hospital and ³Department of Obstetrics and Gynaecology,
10 The University of Melbourne, Parkville 3052, Australia. ⁴Murdoch Children's Research
11 Institute and ⁵Department of Clinical Haematology and ⁶Department of Paediatrics, The
12 Royal Children's Hospital and The University of Melbourne, Parkville 3052, Australia.
13 ⁷Graduate School of Biomedical Engineering, University of New South Wales,
14 Kensington 2033, Australia.

15
16 **Corresponding author:**

17 Dr. Amy Chui
18 NorthWest Academic Centre
19 The University of Melbourne and Sunshine Hospital
20 PO Box 294, 176 Furlong Road
21 St Albans 3021, Australia
22 Tel: +61 3 8395 8088
23 Fax: +61 3 8395 8258
24 Email: akl.chui83@gmail.com

25
26
27
28

29 **Abstract**

30

31 **Objective:**

32 Fetal growth restriction (FGR) is a key cause of adverse pregnancy outcome where
33 maternal and fetal factors are identified as contributing to this condition. Idiopathic FGR
34 is associated with altered vascular endothelial cell functions. Decorin (DCN) has
35 important roles in the regulation of endothelial cell functions in vascular environments.
36 *DCN* expression is reduced in FGR. The objectives were to determine the functional
37 consequences of reduced *DCN* in a human microvascular endothelial cell line model
38 (HMVEC), and to determine downstream targets of *DCN* and their expression in primary
39 placental microvascular endothelial cells (PLECs) from control and FGR-affected
40 placentae.

41 **Approach:**

42 Short-interference RNA was used to reduce *DCN* expression in HMVECs and the effect
43 on proliferation, angiogenesis and thrombin generation was determined. A Growth
44 Factor PCR Array was used to identify downstream targets of *DCN*. The expression of
45 target genes in control and FGR PLECs was performed.

46 **Results:**

47 *DCN* reduction decreased proliferation and angiogenesis but increased thrombin
48 generation with no effect on apoptosis. The array identified three targets of *DCN*:
49 *FGF17*, *IL18* and *MSTN*. Validation of target genes confirmed decreased expression of
50 *VEGFA*, *MMP9*, *EGFR1*, *IGFR1* and *PLGF* in HMVECs and PLECs from control and
51 FGR pregnancies.

52 **Conclusions:**

53 Reduction of *DCN* in vascular endothelial cells leads to disrupted cell functions. The
54 targets of *DCN* include genes that play important roles in angiogenesis and cellular
55 growth. Therefore, differential expression of these may contribute to the pathogenesis of
56 FGR and disease states in other microvascular circulations.

57

58

59 **Key words:** endothelial function; thrombosis; angiogenesis; gene expression;
60 regulation

61

62

63 Introduction

64

65 Fetal growth restriction (FGR) is defined as a neonatal birth-weight less than 10th
66 percentile for gestation together with evidence of fetal welfare compromise such as
67 reduced amniotic fluid volume, increased head to abdomen circumference ratio and
68 abnormal umbilical artery blood flow patterns [1]. FGR greatly increases the risk of
69 perinatal complications including: fetal compromise in labour, fetal death *in utero*,
70 neonatal morbidity and neonatal death [2-4]. Live born infants from pregnancies
71 complicated by FGR have an increased risk of paediatric disorders such as cerebral
72 dysfunction and learning difficulties, and of developing chronic adult onset diseases
73 including: cardiovascular complications, type II diabetes, hypertension and ischemic
74 heart disease [5-7]. Idiopathic FGR accounts for 70% of all cases of FGR and is
75 believed to be associated with uteroplacental insufficiency [8], abnormal umbilical artery
76 Doppler velocimetry [9], oligohydramnios [10] and fetal growth asymmetry [11].
77 Placental insufficiency may result from various factors including: constriction of the
78 placental blood vessels due to reduction in vasodilator activity [12], incomplete
79 cytotrophoblastic invasion of the maternal spiral arteries [13] or maldevelopment of the
80 placental villous structures [14]. These factors result in increased resistance to blood
81 flow within the placenta in both the maternal and fetal circulations, ultimately resulting in
82 fetal hypoxia and acidosis.

83

84 Normal pregnancy represents a hypercoagulable state characterised by profound
85 changes in haemostasis, such as, increased concentration of pro-coagulant factors,
86 decreased anticoagulant activity and diminished fibrinolytic activity [15]. These changes
87 result in increased thrombin generation in maternal plasma and ultimately, increased
88 fibrin formation. These changes in haemostasis ensure the rapid and effective control of
89 bleeding at the time of placental separation during delivery [15]. On the other hand,
90 these changes may also predispose pregnant women to thrombosis and placental
91 vascular complications. Despite this, thrombotic events are rare in uncomplicated
92 pregnancies [16], indicating that thrombin generation must be tightly regulated in this
93 scenario. In contrast, histological examinations of placentae from FGR pregnancies
94 demonstrate increased fibrin deposition and thrombi in the vasculature, including
95 uteroplacental and intervillous thrombosis, perivillous fibrin deposits and villous stem
96 artery thrombosis [16], indicating an increase in overall thrombin activation [17]. The
97 cause of the coagulation disturbance and increased placental thrombosis observed in
98 idiopathic FGR pregnancies is unknown. However, since thrombin generation is
99 significantly increased during normal pregnancy compared to the non-pregnant state
100 [18], the excess thrombin is likely to be generated predominantly by the placenta, as
101 demonstrated by decreased thrombin generation following placental separation during
102 delivery [19].

103

104 Proteoglycans (PGs) are macromolecules comprising a core protein and at least one
105 negatively charged polysaccharide glycosaminoglycan (GAG) side chain. The small
106 leucine-rich proteoglycan (SLRP) family constitutes a network of signal regulation: being
107 mostly extracellular, they are upstream of multiple signalling cascades, a major conduit

108 of information for cellular responses and modulators of distinct pathways [20]. Decorin
109 (DCN) belongs to the Class I SLRPs and can be substituted with one of either
110 chondroitin or dermatan sulphate glycosaminoglycan (GAG) side chains. Previously, we
111 have demonstrated an association between reduced placental *DCN* expression and
112 FGR [21], and propose that due to the many actions of *DCN in vivo*, this reduction
113 contributes to the pathogenesis of FGR [22]. *DCN* and its side chain are involved in
114 multiple biological functions such as, anticoagulation by binding to heparan cofactor II
115 through a highly charged sequence [23], regulation of angiogenic growth factors such
116 as, epidermal growth factor receptor (*EGFR*) and vascular endothelial growth factor
117 (*VEGF*) [24] as well as regulation of basic cellular functions such as proliferation,
118 migration and invasion [25, 26]. Mouse knockout models of *DCN* demonstrate a range
119 of pregnancy disorders including: pre-term birth [27], dystocia and delayed labour onset
120 [28], as well as developmental anomalies in the offspring including: osteoporosis,
121 osteoarthritis and corneal disease [29].
122

123 Since disturbances in many of these biological functions have been demonstrated in the
124 pathogenesis of FGR, *DCN* may in fact play a major role in the pathogenesis of FGR.
125 Therefore, in the present study, we investigated the effect of reduced *DCN* gene
126 expression on the function of microvascular endothelial cells. We also determined the
127 down-stream target genes of *DCN*, in a placental microvascular endothelial cell
128 environment and further validated the expression of these targets in control and FGR-
129 affected placentae.
130
131

132 **Materials and methods (for additional methodology please refer to Supplementary**
133 **Data)**

134
135 **Cell lines**

136 The human microvascular endothelial primary cells from neonatal foreskin (HMVEC)
137 were a kind gift from A/Prof. Grant Drummond (Department of Pharmacology, Monash
138 University).

139
140 **Reduction of DCN expression by siRNA**

141 Four independent *DCN* siRNA oligonucleotides were obtained as “4-For-Silencing
142 siRNA Duplexes”™ (Qiagen, Victoria, Australia). The *DCN* siRNAs showed no
143 significant DNA sequence similarity to other genes in GenBank cDNA databases (data
144 not shown).

145
146 **RNA extraction and cDNA preparation**

147 Total RNA was extracted from cultured HMVECs using PureLink RNA Mini-kits
148 (Lifesciences, Victoria, Australia), as per manufacturer’s instructions. cDNA was
149 prepared in a two-step reaction using 2µg of total RNA.

150
151 **Real-Time PCR**

152 Quantification of *DCN* mRNA expression was determined by real-time PCR in an ABI
153 Prism 7700 (Perkin-Elmer-Applied Biosystems, Victoria, Australia) as described
154 previously [30].

155
156 **Western Immunoblotting**

157 Protein was homogenised and extracted from cultured HMVECs using RIPA Buffer
158 (Pierce, Victoria, Australia). Immunoblotting was performed as described elsewhere
159 [30]. The level of immunoreactive DCN protein relative to GAPDH was determined
160 semi-quantitatively using scanning densitometry (Image Quant, New South Wales,
161 Australia).

162
163 **HMVEC cell growth using xCELLigence**

164 HMVEC cell growth was assessed using the xCELLigence SP real-time system (Roche
165 Diagnostics, Victoria, Australia) according to the manufacturer’s instructions. The results
166 were analysed using the RTCA Software 1.2 (Roche Diagnostics, Victoria, Australia)
167 and GraphPad Prism 5 (GraphPad Software, California, USA).

168
169 **HMVEC network formation assays**

170 HMVEC network formation was assessed using the µ-Slide Angiogenesis system (IBIDI,
171 Victoria, Australia) as per manufacturer’s instructions using 10µl of neat Growth-Factor
172 Reduced Matrigel™ (BD, Victoria, Australia). Photomicrographs of entire wells were
173 taken in triplicates and branch points were counted by Wimasis Image Analysis.

174
175 **Thrombin Generation Assays**

176 HMVECs were plated into 96 well plates at a density of 5000 cells per well and
177 transfected with *DCN* siRNAs and controls for 48h. Venous blood was collected from

178 healthy blood donors (n=40). Measurement of endogenous thrombin potential (ETP) by
179 Calibrated Automated Thrombogram (CAT, Thrombinoscope, Stago Diagnostica,
180 Victoria, Australia) was performed according to manufacturer's instructions. The ETP
181 (nM/minute) was calculated using the Thrombinoscope software version 3.0.0.29.
182

183 **Human Growth Factors PCR Array**

184 The "Human Growth Factor" Taqman PCR array (Applied Biosystems, Victoria, Australia)
185 for gene profiling was used to screen for downstream target genes of *DCN*, according to
186 manufacturer's instructions. Candidate genes were prioritised based on level of gene
187 expression i.e. at least 2-fold change in mRNA expression in siRNA treated cells when
188 compared with NC.
189

190 **Feto-placental microvascular endothelial cell (PLEC) isolation**

191 Placentae from pregnancies complicated by idiopathic FGR (n=3) and gestation-
192 matched control (n=3) pregnancies were collected with informed patient consent and
193 approval from the Human Research and Ethics Committees of The Royal Women's
194 Hospital, Melbourne. Ultrasound data were used to prospectively identify pregnancies
195 complicated by FGR. The inclusion criteria of patients included in this study has been
196 previously published [21].
197

198 Isolation of PLECs was undertaken according to the published methods of Dunk et al.
199 2012, using placental biopsies obtained from fresh placenta [31].
200

201 **Data Analysis**

202 All data in this study are described as mean±SEM and analysed by the GraphPad Prism
203 6 statistical software (GraphPad Software, California, USA). One-Way ANOVA was
204 used to assess the differences in *DCN* mRNA and protein expression between siRNA-
205 treated and control groups as well as in HMVEC functional assay studies. The Mann-
206 Whitney U test was used to analyse differences in gene expression between whole
207 placenta and PLECs from control and FGR-affected placentae. A probability value of
208 <0.05 was considered significant.
209

210 **Results**

211 **Reduced *DCN* mRNA and protein expression following siRNA transfection in 212 HMVECs**

213 Four independent siRNAs (designated as siRNA1-4), were designed to reduce *DCN*
214 expression in HMVECs. A non-siRNA transfected control (Mock) and a non-specific
215 siRNA transfected control were used as negative controls. Fig 1A revealed that
216 treatment with siRNA2 and siRNA3 significantly reduced *DCN* mRNA expression
217 compared to both the Mock and NC controls (Mock: 0.90±0.14 and NC: 0.59±0.02 vs.
218 s2: 0.01±0.001 and s3: 0.05±0.01, p<0.005, n=18, One-Way ANOVA) at 48h after
219 transfection. A representative immunoblot for *DCN* (60kDa) protein is shown in Fig 1B
220 for Mock, NC, siRNA2 and siRNA3, with the corresponding GAPDH. Semi-quantitative
221 densitometry analysis revealed a decrease in immunoreactive *DCN* protein abundance
222
223

224 in HMVECs treated with siRNA2 or siRNA3 compared with both the Mock and NC
225 controls (Mock: 1.76 ± 0.05 and NC: 1.57 ± 0.05 vs. s2: 0.10 ± 0.01 and s3: 0.08 ± 0.1 ,
226 $p < 0.05$, $n = 3$, One-Way ANOVA, Fig 1C).

227

228 **Reduced *DCN* expression does not increase HMVEC apoptosis**

229 In order to determine that the reduction in *DCN* expression was not due to apoptosis as
230 a result of treatment with siRNAs, the mRNA expression of three common apoptotic
231 markers were analysed. Real-time PCR revealed that the mRNA expression of *BCL2*,
232 *p53* and *CASPASE3* were not significantly different compared to the Mock or the NC
233 controls ($p > 0.05$, $n = 18$, One-Way ANOVA, data not shown).

234

235 **Reduced *DCN* expression decreases HMVEC proliferation and network formation 236 but increases thrombin generation**

237 The effect on HMVEC proliferation after 48h *DCN* siRNA2 or siRNA3 treatment was
238 determined using the xCELLigence system. Optimisation experiments confirmed that
239 5000 cells per well was the optimal density of cells to allow uninhibited cell proliferation
240 (data not shown). Fig 2A is a representative graph showing the cell index of HMVECs
241 treated with siRNA compared to Mock or NC controls over 72h. At 48h post-siRNA
242 transfection, the proliferation potential of the HMVECs were significantly decreased
243 following *DCN* reduction compared to both controls (Mock: 1.92 ± 0.04 and NC:
244 1.94 ± 0.02 vs. s2: 1.19 ± 0.06 and s3: 1.25 ± 0.26 , $p < 0.05$, $n = 18$, One-Way ANOVA, Fig
245 2B).

246

247 The ability of HMVECs to form networks after *DCN* gene reduction was determined
248 using the μ -slide Angiogenesis system by IBIDI. Optimisation experiments to determine
249 the optimal Growth-Factor Reduced Matrigel™ concentration and cell density were
250 performed (data not shown). Following incubation for 48h, the cells were stained with
251 calcein. Fig 2C shows representative images at 100x magnification taken after 48h *DCN*
252 siRNA transfection and reveals a qualitative decrease in HMVEC network formation
253 compared to Mock or NC controls. Branch points were analysed and revealed that the
254 network formation potential of HMVECs were significantly decreased following *DCN*
255 gene reduction compared to Mock and NC controls (Mock: 9.0 ± 0.62 and NC: 9.27 ± 0.63
256 vs. s2: 2.36 ± 0.59 and s3: 4.09 ± 0.89 , $p < 0.01$, $n = 18$, One-Way ANOVA, Fig 2D).

257

258 The ETP of the HMVECs following the reduction in *DCN* gene expression was
259 determined using the CAT system. A representative thrombin generation curve following
260 reduction in *DCN* gene expression in HMVECs is depicted in Fig 2E. Reduction of *DCN*
261 expression by siRNA3 resulted in a significant increase in the ETP of the HMVECs
262 compared with the Mock and NC controls (Mock: 1757.83 ± 152.98 and NC:
263 1749.28 ± 40.66 vs. s3: 1903.44 ± 107.33 , $p < 0.03$, $n = 9$, One-Way ANOVA, Fig 2F).

264

265 **Identification of *DCN* downstream target genes**

266 HMVECs were transfected with a NC control and siRNA3 and the “Human Growth
267 Factors” Taqman PCR array was used to identify potential downstream target genes of
268 *DCN*. The relative mRNA expression of the 84 genes after *DCN* mRNA and protein
269 down-regulation is shown in Fig 3. The Y-axis represents the fold change for each of the

270 84 genes normalised to the average expression of the five housekeeping genes
271 included in the array. Genes that had an expression level above the positive two-fold
272 change as indicated by a red line, was classified as genes with a fold increase.
273 Conversely, genes that had an expression level below the negative two-fold change
274 green line were classified as genes with a fold decrease in gene expression. The
275 screening array identified three potential candidate downstream target genes of *DCN* in
276 HMVECs. These are fibroblast growth factor 17 (*FGF17*) with a fold increase of 2.4,
277 interleukin 18 (*IL18*) with a fold decrease of 3.3 and myostatin (*MSTN*) with a fold
278 decrease of -2.8.

279
280 The mRNA expression of *FGF17*, *IL18*, and *MSTN* were further validated in HMVECs
281 transfected with *DCN* siRNA independently (Fig 4). Increased expression of *FGF17*
282 (Mock: 1.04 ± 0.19 and NC: 1.29 ± 0.14 vs. s2: 4.62 ± 0.76 and s3: 4.77 ± 0.46 , $p < 0.05$, $n = 9$,
283 One-Way ANOVA) and decreased expression of *MSTN* (Mock: 1.00 ± 0.06 and NC:
284 1.81 ± 0.18 vs. s2: 0.51 ± 0.19 and s3: 0.43 ± 0.09 , $p < 0.05$, $n = 9$, One-Way ANOVA) was
285 confirmed. *IL18* was not differentially expressed in *DCN* reduced HMVECs under
286 independent validation (data not shown).

287
288 The mRNA expression of known target genes of *DCN* from the published literature was
289 also investigated in HMVECs following *DCN* gene reduction. As shown in Fig 5, the
290 expression of *VEGFA* (Mock: 1.21 ± 0.11 and NC: 1.01 ± 0.10 vs. s2: 0.40 ± 0.05 and s3:
291 0.18 ± 0.07 , $p < 0.05$, $n = 9$, One-Way ANOVA), *MMP9* (Mock: 1.19 ± 0.21 and NC: 0.85
292 ± 0.11 vs. s2: 0.14 ± 0.01 and s3: 0.03 ± 0.02 , $p < 0.01$, $n = 9$, One-Way ANOVA), *EGFR1*
293 (Mock: 0.76 ± 0.22 and NC: 1.00 ± 0.01 vs. s2: 0.26 ± 0.03 and s3: 0.18 ± 0.03 , $p < 0.05$, $n = 9$,
294 One-Way ANOVA), *IGFR1* (Mock: 0.80 ± 0.06 and NC: 1.01 ± 0.11 vs. s2: 0.41 ± 0.06 and
295 s3: 0.29 ± 0.03 , $p < 0.05$, $n = 9$, One-Way ANOVA) and *PLGF* (Mock: 1.07 ± 0.27 and NC:
296 1.96 ± 0.06 vs. s2: 0.23 ± 0.02 and s3: 0.28 ± 0.05 , $p < 0.03$, $n = 9$, One-Way ANOVA) were
297 significantly reduced following treatment with *DCN* siRNA2 or siRNA3 compared with
298 the Mock or NC controls. The mRNA expression of *MMP2*, *HIF1A*, *Thrombospondin1*,
299 *TIMP3*, *TLR2* and *TLR4* were not significantly different between the two groups (data
300 not shown).

301 302 **Validation of *DCN* and its downstream target genes in control and FGR-affected** 303 **primary placental endothelial cells (PLECs)**

304 The mRNA expression of *DCN* and its targets were validated in PLECs cultured from
305 control and FGR-affected placentae. Shown in Fig 6A, the mRNA expression of *DCN*
306 was significantly decreased in PLECs cultured from FGR-affected placentae compared
307 with controls (Control PLEC: 1.04 ± 0.14 vs. FGR PLEC: 0.21 ± 0.06 , $p < 0.003$, $n = 3$ each,
308 Mann-Whitney U Test). In Fig 6B-F, significant decreases in mRNA expression was also
309 observed for *EGFR1* (Control PLEC: 1.04 ± 0.11 vs. FGR PLEC: 0.26 ± 0.06 , $p < 0.003$,
310 $n = 3$ each, Mann-Whitney U Test), *IGFR1* (Control PLEC: 1.05 ± 0.15 vs. FGR PLEC:
311 0.45 ± 0.05 , $p < 0.005$, $n = 3$ each, Mann-Whitney U Test), *PLGF* (Control PLEC: 1.18 ± 0.32
312 vs. FGR PLEC: 0.32 ± 0.12 , $p < 0.05$, $n = 3$ each, Mann-Whitney U Test) and *VEGFA*
313 (Control PLEC: 1.52 ± 0.60 vs. FGR PLEC: 0.33 ± 0.07 , $p < 0.05$, $n = 3$ each, Mann-Whitney
314 U Test) between control and FGR-affected PLECs. In contrast, the mRNA expression of
315 *MMP9* was significantly increased in FGR-affected PLECs compared with controls

316 (Control PLEC: 1.09 ± 0.21 vs. FGR PLEC: 2.51 ± 0.40 , $p < 0.03$, $n=3$ each, Mann-Whitney
317 U Test). These results are consistent with those observed in the previous validation
318 experiments using HMVECs (with the exception of FGF17 and MSTN which were not
319 expressed in PLECs).
320
321

ACCEPTED MANUSCRIPT

322 Discussion

323

324 In this current study we focused on *DCN*, a small leucine-rich proteoglycan, and
325 demonstrate for the first time that reduction of *DCN* gene expression in a primary
326 human microvascular endothelial cell type (HMVEC) results in a significant decrease in
327 HMVEC proliferation, network formation and thrombin generation. We also revealed
328 differential expression of *DCN* target genes in FGR-affected primary placental
329 microvascular endothelial cells (PLECs). The results reveal a consistency in the
330 expression patterns of *VEGFA*, *MMP9*, *EGFR1*, *IGFR1* and *PLGF*.

331

332 In tumour cells, *DCN* has been shown to command a powerful anti-tumorigenic signal
333 by potently repressing and attenuating tumour cell proliferation, survival, migration and
334 angiogenesis via binding to *EGFR* and *IGFR* [32]. In addition, *DCN* has also been
335 described as an angiostatic agent in tumour cells via a reduction in *VEGF* and *MMP9*
336 production [33]. In extravillous trophoblast cells, *DCN* has been shown to be an
337 antagonist of proliferation and migration, via suppression of *VEGFR2* and *EGFR1* [25],
338 as well as extravillous differentiation and angiogenesis by blocking activation of p38
339 MAPK, and ERK pathways by *VEGFA* [34].

340

341 In this study, reduction of *DCN* expression resulted in decreased HMVEC proliferation
342 and network formation, potentially due to the subsequent downstream decrease in the
343 expression of *EGFR1*, *IGFR1* and *VEGFR*. Inadequate fetal vessel angiogenesis and
344 proliferation is consistent with histological observations of the FGR placenta [14]. Thus
345 *DCN* appears to mediate a pro-angiogenic role in HMVECs and deficiency of *DCN*
346 results in inhibition of angiogenesis and proliferation. Our findings are in contrast with
347 those in the cancer literature but are supported by other studies demonstrating a pro-
348 angiogenic and pro-proliferative response of *DCN*, primarily on normal, non-tumorigenic
349 endothelial cells [35]. Furthermore, evidence suggests that *DCN*-deficient mice have
350 diminished growth of vessels [36].

351

352 Despite the multiple biological actions of *DCN* on a variety of cell types, the nature of
353 the cell surface receptors responsible for *DCN* action has remained elusive in many
354 cases. For example, *DCN* was shown to interact with *EGFR* in a squamous cell
355 carcinoma line, leading to the triggering of a signal cascade, and finally growth
356 suppression associated with a retardation of *EGFR* recycling to the cell surface [37-41].
357 *DCN* also interacts with *IGFR* in endothelial cells, leading to its phosphorylation,
358 followed by a down-regulation of the receptor, resulting in cell survival [25]. Therefore,
359 the dichotomous effect reported for *DCN* on endothelial cells and the previously
360 described function on tumourigenesis creates a scenario where *DCN* may be able to
361 differentially modulate angiogenesis.

362

363 Another plausible explanation for the diverse functions of *DCN* is that small leucine-rich
364 proteoglycans undergo a dimer-monomer transition that would expose key sites
365 involved in specific bindings; therefore their functional activity *in vivo* would be regulated
366 by the structure of *DCN* in that particular cell type and by the intrinsic affinity of *DCN* for

367 its cognate receptor [20, 42]. In addition, the binding and function of DCN to specific
368 receptors also depends on whether it is a GAG-bound DCN or just the core protein [43].
369

370 The differences between the cells in the previous published work are that both tumour
371 cells and extravillous trophoblast cells are highly proliferative, invasive and angiogenic
372 where *DCN* negatively regulates angiogenesis and proliferation in highly proliferative,
373 invasive, and angiogenic environment to prevent aberrant tumour growth. However, in
374 this study, we used HMVECs, which represents normal microvascular environment
375 whose primary function is to form networks during vascular development. Therefore, it is
376 possible that in a normal microvasculature environment, where a balanced level of
377 angiogenesis and proliferation is required, *DCN* may act positively to regulate
378 proliferation and angiogenesis.
379

380 Thrombin generation is a global haemostatic functional assay used widely to measure
381 hypo- or hyper-coagulability and reflects the interplay of all haemostatic factors in
382 plasma/blood. The ETP provides an *in vitro* measure of the overall ability to generate
383 thrombin, the final crucial stage of haemostasis and is therefore, the best assessment of
384 global haemostasis [44]. The ETP quantifies the visual differences between the
385 thrombin generation curves and allows for statistical analysis. This study has
386 demonstrated a modest, but statistically significant increase in thrombin generation
387 following reduction in *DCN* expression in HMVECs which implies a hyper-coagulable
388 state with *DCN* down-regulation. This is consistent with observations in the FGR
389 placenta where increased intervillous thrombi are observed [9]. Delorme et al (1998)
390 isolated and characterized the glycosaminoglycan, dermatan sulphate (DS), in term
391 human placenta and revealed that DS was predominantly present on the protein core of
392 DCN. Since DS catalyzes the inhibition of thrombin by heparin-cofactor II [45], a
393 reduction in *DCN* expression in HMVECs could result in an increase in thrombin
394 generation [19]. Although the difference observed is small, this difference in a *global*
395 setting could potentially lead to significant changes to overall thrombin generation in the
396 placental microvascular system. It is therefore plausible that the observed increase in
397 localised placental intravascular thrombosis is due to a decrease in the expression of
398 *DCN* in human FGR-affected placentae [21].
399

400 Since it appears that the molecular function of DCN is also highly dependent on the
401 structure, function and sulfation/glycosylation sites of both the protein core and the GAG
402 side chain [20, 46, 47], investigations into the exact structural moiety of DCN in both the
403 control and FGR-affected placenta could reveal important information about the role of
404 DCN in the pathogenesis of FGR.
405

406 In summary, this study has shown that reduced expression of the proteoglycan *DCN* in
407 a microvascular endothelial cell line results in altered endothelial cell functions such as
408 proliferation and network formation as well as an increase in global thrombin generation
409 without affecting apoptosis. These alterations may be a consequence of altered growth
410 factor expression as a result of downstream regulation by *DCN* or via a direct local
411 effect of reduced *DCN* and dermatan sulphate abundance. These findings provide
412 valuable insight into the endothelial milieu in the growth restricted placenta. This raises

413 the possibility that increased *DCN* expression may improve the anti-angiogenic and
414 thrombotic changes observed within the placental vasculature in FGR. Moreover, the
415 findings of this study have implications beyond pregnancy and suggest that *DCN* may
416 play important roles in the pathogenesis of other disease states in microvascular
417 circulations through these angiogenic, thrombotic and growth factor mediated pathways.

418
419 In addition, investigation of the relative roles of the DCN protein core versus the GAG
420 side chain in these functions may assist in revealing the logical therapeutic approaches
421 to the treatment of FGR and related vascular pathologies.
422

423 **Acknowledgements**

424

425 **a)** The authors would like to thank Diagnostica Stago (Australia) for the loan of the
426 Calibrated Automated Thrombogram.

427

428 **b)** Sources of funding: this work was supported by a National Health and Medical
429 Research Council (NH&MRC) Project Grant, Australia (Application: 1004952).

430

431

ACCEPTED MANUSCRIPT

432 **References**

- 433
- 434 [1]. Mongelli M, Gardosi J. Fetal growth. *Curr Opin Obstet Gynecol*. 2000;12(2):111-
435 5.
- 436 [2]. McIntire DD, Bloom SL, Casey BM, Leveno KJ. Birth weight in relation to
437 morbidity and mortality among newborn infants. *N Engl J Med*. 1999;340(16):1234-8.
- 438 [3]. Kramer MS, Olivier M, McLean FH, Willis DM, Usher RH. Impact of intrauterine
439 growth retardation and body proportionality on fetal and neonatal outcome. *Pediatrics*.
440 1990;86(5):707-13.
- 441 [4]. Froen JF, Gardosi JO, Thurmann A, Francis A, Stray-Pedersen B. Restricted
442 fetal growth in sudden intrauterine unexplained death. *Acta Obstet Gynecol Scand*.
443 2004;83(9):801-7.
- 444 [5]. Rosso IM, Cannon TD, Huttunen T, Huttunen MO, Lonqvist J, Gasperoni TL.
445 Obstetric risk factors for early-onset schizophrenia in a Finnish birth cohort. *Am J*
446 *Psychiatry*. 2000;157(5):801-7.
- 447 [6]. Godfrey KM, Barker DJ. Fetal nutrition and adult disease. *Am J Clin Nutr*.
448 2000;71(5 Suppl):1344S-52S.
- 449 [7]. Godfrey KM, Barker DJ. Fetal programming and adult health. *Public Health Nutr*.
450 2001;4(2B):611-24.
- 451 [8]. Ghidini A. Idiopathic fetal growth restriction: a pathophysiologic approach. *Obstet*
452 *Gynecol Surv*. 1996;51(6):376-82.
- 453 [9]. Salafia CM, Pezzullo JC, Minior VK, Divon MY. Placental pathology of absent
454 and reversed end-diastolic flow in growth-restricted fetuses. *Obstet Gynecol*.
455 1997;90(5):830-6.
- 456 [10]. Volante E, Gramellini D, Moretti S, Kaihura C, Bevilacqua G. Alteration of the
457 amniotic fluid and neonatal outcome. *Acta Biomed*. 2004;75 Suppl 1:71-5.
- 458 [11]. Vik T, Markestad T, Ahlsten G, Gebre-Medhin M, Jacobsen G, Hoffman HJ, et al.
459 Body proportions and early neonatal morbidity in small-for-gestational-age infants of
460 successive births. *Acta Obstet Gynecol Scand Suppl*. 1997;165:76-81.
- 461 [12]. Chang TC, Robson SC, Spencer JA, Gallivan S. Identification of fetal growth
462 retardation: comparison of Doppler waveform indices and serial ultrasound
463 measurements of abdominal circumference and fetal weight. *Obstet Gynecol*.
464 1993;82(2):230-6.
- 465 [13]. Gagnon R. Placental insufficiency and its consequences. *Eur J Obstet Gynecol*
466 *Reprod Biol*. 2003;110 Suppl 1:S99-107.
- 467 [14]. Kingdom J, Huppertz B, Seaward G, Kaufmann P. Development of the placental
468 villous tree and its consequences for fetal growth. *Eur J Obstet Gynecol Reprod Biol*.
469 2000;92(1):35-43.
- 470 [15]. Brenner B. Haemostatic changes in pregnancy. *Thromb Res*. 2004;114(5-6):409-
471 14.
- 472 [16]. Lanir N, Aharon A, Brenner B. Haemostatic mechanisms in human placenta.
473 *Best practice & research Clinical haematology*. 2003;16(2):183-95. Epub 2003/05/24.
- 474 [17]. Kingdom JC, Kaufmann P. Oxygen and placental villous development: origins of
475 fetal hypoxia. *Placenta*. 1997;18(8):613-21; discussion 23-6.

- 476 [18]. Uszynski M. Generation of thrombin in blood plasma of non-pregnant and
477 pregnant women studied through concentration of thrombin-antithrombin III complexes.
478 *Eur J Obstet Gynecol Reprod Biol.* 1997;75(2):127-31.
- 479 [19]. Delorme MA, Xu L, Berry L, Mitchell L, Andrew M. Anticoagulant dermatan
480 sulfate proteoglycan (decorin) in the term human placenta. *Thromb Res.*
481 1998;90(4):147-53. Epub 1998/08/06.
- 482 [20]. Schaefer L, Iozzo RV. Biological functions of the small leucine-rich
483 proteoglycans: from genetics to signal transduction. *J Biol Chem.* 2008;283(31):21305-
484 9. Epub 2008/05/09.
- 485 [21]. Swan BC, Murthi P, Rajaraman G, Pathirage NA, Said JM, Ignjatovic V, et al.
486 Decorin expression is decreased in human idiopathic fetal growth restriction. *Reprod*
487 *Fertil Dev.* 2010;22(6):949-55. Epub 2010/07/02.
- 488 [22]. Said JM. The role of proteoglycans in contributing to placental thrombosis and
489 fetal growth restriction. *J Pregnancy.* 2011;2011:928381. Epub 2011/04/15.
- 490 [23]. Chen J, Liu J. Characterization of the structure of antithrombin-binding heparan
491 sulfate generated by heparan sulfate 3-O-sulfotransferase 5. *Biochim Biophys Acta.*
492 2005;1725(2):190-200. Epub 2005/08/16.
- 493 [24]. Reinboth B, Thomas J, Hanssen E, Gibson MA. Beta ig-h3 interacts directly with
494 biglycan and decorin, promotes collagen VI aggregation, and participates in ternary
495 complexing with these macromolecules. *J Biol Chem.* 2006;281(12):7816-24. Epub
496 2006/01/26.
- 497 [25]. Iacob D, Cai J, Tsonis M, Babwah A, Chakraborty C, Bhattacharjee RN, et al.
498 Decorin-mediated inhibition of proliferation and migration of the human trophoblast via
499 different tyrosine kinase receptors. *Endocrinology.* 2008;149(12):6187-97.
- 500 [26]. Xu G, Guimond MJ, Chakraborty C, Lala PK. Control of proliferation, migration,
501 and invasiveness of human extravillous trophoblast by decorin, a decidual product. *Biol*
502 *Reprod.* 2002;67(2):681-9.
- 503 [27]. Calmus ML, Macksoud EE, Tucker R, Iozzo RV, Lechner BE. A mouse model of
504 spontaneous preterm birth based on the genetic ablation of biglycan and decorin.
505 *Reproduction.* 2011;142(1):183-94. Epub 2011/04/20.
- 506 [28]. Meyerson M, Counter CM, Eaton EN, Ellisen LW, Steiner P, Caddle SD, et al.
507 hEST2, the putative human telomerase catalytic subunit gene, is up-regulated in tumor
508 cells and during immortalization. *Cell.* 1997;90(4):785-95. Epub 1997/08/22.
- 509 [29]. Gimbrone MA, Jr., Fareed GC. Transformation of cultured human vascular
510 endothelium by SV40 DNA. *Cell.* 1976;9(4 PT 2):685-93. Epub 1976/12/01.
- 511 [30]. Chui A, Zainuddin N, Rajaraman G, Murthi P, Brennecke SP, Ignjatovic V, et al.
512 Placental syndecan expression is altered in human idiopathic fetal growth restriction.
513 *Am J Pathol.* 2012;180(2):693-702. Epub 2011/12/06.
- 514 [31]. Dunk CE, Roggensack AM, Cox B, Perkins JE, Asenius F, Keating S, et al. A
515 distinct microvascular endothelial gene expression profile in severe IUGR placentas.
516 *Placenta.* 2012;33(4):285-93. Epub 2012/01/24.
- 517 [32]. Neill T, Painter H, Buraschi S, Owens RT, Lisanti MP, Schaefer L, et al. Decorin
518 antagonizes the angiogenic network: concurrent inhibition of Met, hypoxia inducible
519 factor 1alpha, vascular endothelial growth factor A, and induction of thrombospondin-1
520 and TIMP3. *J Biol Chem.* 2012;287(8):5492-506. Epub 2011/12/24.

- 521 [33]. Neill T, Schaefer L, Iozzo RV. Decorin: a guardian from the matrix. *Am J Pathol.*
522 2012;181(2):380-7. Epub 2012/06/28.
- 523 [34]. Lala N, Girish GV, Cloutier-Bosworth A, Lala PK. Mechanisms in decorin
524 regulation of vascular endothelial growth factor-induced human trophoblast migration
525 and acquisition of endothelial phenotype. *Biol Reprod.* 2012;87(3):59. Epub 2012/06/16.
- 526 [35]. Nelimarkka L, Salminen H, Kuopio T, Nikkari S, Ekfors T, Laine J, et al. Decorin
527 is produced by capillary endothelial cells in inflammation-associated angiogenesis. *Am J*
528 *Pathol.* 2001;158(2):345-53. Epub 2001/02/13.
- 529 [36]. Schonherr E, Sunderkotter C, Schaefer L, Thanos S, Grassel S, Oldberg A, et al.
530 Decorin deficiency leads to impaired angiogenesis in injured mouse cornea. *J Vasc*
531 *Res.* 2004;41(6):499-508. Epub 2004/11/06.
- 532 [37]. Csordas G, Santra M, Reed CC, Eichstetter I, McQuillan DJ, Gross D, et al.
533 Sustained down-regulation of the epidermal growth factor receptor by decorin. A
534 mechanism for controlling tumor growth in vivo. *J Biol Chem.* 2000;275(42):32879-87.
535 Epub 2000/07/27.
- 536 [38]. Iozzo RV, Moscatello DK, McQuillan DJ, Eichstetter I. Decorin is a biological
537 ligand for the epidermal growth factor receptor. *J Biol Chem.* 1999;274(8):4489-92.
538 Epub 1999/02/13.
- 539 [39]. Patel S, Santra M, McQuillan DJ, Iozzo RV, Thomas AP. Decorin activates the
540 epidermal growth factor receptor and elevates cytosolic Ca²⁺ in A431 carcinoma cells.
541 *J Biol Chem.* 1998;273(6):3121-4. Epub 1998/03/07.
- 542 [40]. Santra M, Reed CC, Iozzo RV. Decorin binds to a narrow region of the epidermal
543 growth factor (EGF) receptor, partially overlapping but distinct from the EGF-binding
544 epitope. *J Biol Chem.* 2002;277(38):35671-81. Epub 2002/07/10.
- 545 [41]. Zhu JX, Goldoni S, Bix G, Owens RT, McQuillan DJ, Reed CC, et al. Decorin
546 evokes protracted internalization and degradation of the epidermal growth factor
547 receptor via caveolar endocytosis. *J Biol Chem.* 2005;280(37):32468-79. Epub
548 2005/07/05.
- 549 [42]. McEwan PA, Scott PG, Bishop PN, Bella J. Structural correlations in the family of
550 small leucine-rich repeat proteins and proteoglycans. *J Struct Biol.* 2006;155(2):294-
551 305. Epub 2006/08/04.
- 552 [43]. Fiedler LR, Schonherr E, Waddington R, Niland S, Seidler DG, Aeschlimann D,
553 et al. Decorin regulates endothelial cell motility on collagen I through activation of
554 insulin-like growth factor I receptor and modulation of alpha2beta1 integrin activity. *J*
555 *Biol Chem.* 2008;283(25):17406-15. Epub 2008/04/17.
- 556 [44]. Al Dieri R, Peyvandi F, Santagostino E, Giansily M, Mannucci PM, Schved JF, et
557 al. The thrombogram in rare inherited coagulation disorders: its relation to clinical
558 bleeding. *Thromb Haemost.* 2002;88(4):576-82. Epub 2002/10/04.
- 559 [45]. Tollefsen DM, Pestka CA, Monafó WJ. Activation of heparin cofactor II by
560 dermatan sulfate. *J Biol Chem.* 1983;258(11):6713-6. Epub 1983/06/10.
- 561 [46]. Moreth K, Iozzo RV, Schaefer L. Small leucine-rich proteoglycans orchestrate
562 receptor crosstalk during inflammation. *Cell Cycle.* 2012;11(11):2084-91. Epub
563 2012/05/15.
- 564 [47]. Schaefer L, Schaefer RM. Proteoglycans: from structural compounds to signaling
565 molecules. *Cell Tissue Res.* 2010;339(1):237-46. Epub 2009/06/11.
- 566

567
568
569
570
571
572
573
574
575
576
577
578
579
580
581
582
583
584
585
586
587
588
589
590
591
592
593
594
595
596
597
598
599
600
601
602
603
604
605
606
607
608
609
610
611
612

Figure legends

Figure 1 Reduced *DCN* mRNA and protein expression following siRNA transfection in HMVECs

A. Real-time PCR was performed on HMVECs transfected with Mock and NC control, *DCN* siRNA1, 2, 3 and 4 oligonucleotides, over 24, 48 and 72 hours. Relative quantification of *DCN* mRNA expression relative to the housekeeping gene *18S rRNA* was calculated using the $2^{-\Delta\Delta CT}$ method. * = Significance, $p < 0.05$, $n = 18$, One-Way ANOVA. The Y-axis represents the mRNA expression of decorin relative to *18S rRNA*.

B. Protein was extracted from cultured HMVECs after transfection with Mock and NC control and *DCN* siRNA2 or siRNA3 oligonucleotides for 48 hours. Protein samples (25 μ g) were electrophoresed on a 10% SDS-PAGE gel and transferred to a PVDF membrane. Immunoblotting was performed and chemiluminescent detection of the 60kDa *DCN* protein is shown in the upper panel. Lanes 1, 2, 3 and 4 represents the Mock and NC control, *DCN* siRNA3 and siRNA4 transfected samples in HMVECs, respectively. The lower panel is GAPDH showing the protein load for all samples.

C. The densitometric values normalised to GAPDH for *DCN* immunoreactive protein after siRNA transfection in HMVECs is shown. * = Significance, $p < 0.05$, $n = 3$, One-Way ANOVA. The Y-axis represents the densitometric values of decorin protein relative to GAPDH.

Figure 2 Reduced *DCN* expression decreases HMVEC proliferation and network formation but increases thrombin generation

A. HMVEC proliferation was determined using xCELLigence (Roche Diagnostics, USA). A representative graph showing the cell index (Y-axis) of HMVECs transfected with Mock, NC, *DCN* siRNA2 or siRNA3 over a 72h time period is presented here.

B. The total effect of *DCN* gene reduction on HMVEC proliferation was determined quantitatively at the 48h time-point. * = Significance, $p < 0.05$, $n = 18$, One-Way ANOVA. The Y-axis represents the cell index over time.

C. Representative images of HMVEC network formation after 48h Mock, NC, and *DCN* siRNA2 or siRNA3 transfection. Cells were stained with calcein and images were taken using a fluorescent microscope (CellIR, Olympus, Japan). Magnification of all images is at 100X, scale bars represent 50 μ m.

D. The ability for HMVECs to form networks after transfection with Mock, NC, *DCN* siRNA2 or siRNA3 over a 48h time period was determined using IBIDI angiogenesis slides (IBIDI, Germany). The total number of branch points was determined using the Wimasis Image Analysis tool. * = Significance, $p < 0.05$, $n = 18$, One-Way ANOVA. The Y-axis represents the number of branch points at 48h.

E. A representative thrombin generation curve showing the effect of *DCN* gene reduction in HMVECs is shown here. The Y-axis represents the amount of thrombin generated relative to time.

F. A statistical representation of the effect of reduced *DCN* expression on the ETP of HMVECs is shown. * = Significance, $p < 0.05$, $n = 9$, One-Way ANOVA. The Y-axis represents the amount of thrombin generated relative to time.

613 **Figure 3 Identification of *DCN* downstream target genes after siRNA transfection**
614 RNA was extracted from HMVECs transfected with *DCN* siRNA, transcribed into first
615 strand cDNA, and the Taqman Growth Factors Real-time PCR array was performed for
616 gene profiling. The 84 pre-dispensed genes, which included a panel of housekeeping
617 genes, were amplified for 40 cycles of denaturation and primer extension. Gene
618 expression values (fold change above or below threshold value of 2) were subsequently
619 calculated for the *DCN* siRNA-treated plate, relative to the NC control and normalised to
620 the housekeeping gene panel (x-axis). The red line shows the threshold value at 2 and
621 the green line shows the threshold value at -2. Values greater than 2 were termed a fold
622 increase and those less than -2 were considered a fold decrease.

623
624 **Figure 4 Validation of candidate *DCN* downstream target genes in cultured**
625 **HMVECs**

626 cDNA from HMVECs transfected with Mock and NC controls, and *DCN* siRNA2 or
627 siRNA3 were amplified for 40 cycles using pre-validated Taqman gene expression
628 assays for *FGF17* (A) and *MSTN* (B). The *18S rRNA* housekeeping gene was used for
629 relative quantification according to the $2^{-\Delta\Delta CT}$ method of Livak and Schmittgen (2001).
630 The NC control was used as the calibrator. * = Significance, $p < 0.05$, $n = 9$, One-Way
631 ANOVA. The Y-axis represents the gene expression relative to *18S rRNA*.

632
633 **Figure 5 Expression of candidate target genes of *DCN* in HMVECs after reduction**
634 **in *DCN* expression**

635 The mRNA expression of *VEGFA* (A), *MMP9* (B), *EGFR* (C), *IGFR1*
636 (D) and *PLGF* (E) was determined by real-time PCR using pre-validated
637 Taqman gene expression assays. The *18S rRNA* housekeeping gene was used for
638 relative quantification according to the $2^{-\Delta\Delta CT}$ method of Livak and Schmittgen (2001).
639 The NC control was used as the calibrator. * = Significance, $p < 0.05$, $n = 9$, One-Way
640 ANOVA. The Y-axis represents the gene expression relative to *18S rRNA*.

641
642 **Figure 6 Expression of *DCN* and its target genes in control and FGR-affected**
643 **primary placental endothelial cells**

644 The mRNA expression of *DCN*, *EGFR1*, *IGFR1*, *PLGF*, *VEGFA* and *MMP9* was
645 determined by real-time PCR according to the $2^{-\Delta\Delta CT}$ method of Livak and Schmittgen
646 (2001). The control PLECs were used as the calibrator. * = Significance, $p < 0.05$, Mann-
647 Whitney U Test. The Y-axis represents the gene expression relative to *18S rRNA*.
648

649
650
651
652
653
654
655
656
657
658
659
660
661
662
663
664
665
666
667
668
669
670
671
672
673
674
675
676
677
678
679

Author Contributions

1. Chui, A – I declare that I participated in the study design, performing of all experiments, data analysis and interpretation, writing of manuscript and final approval of manuscript for submission.
2. Murthi, P- I declare that I participated in the study concept and design, performed the isolation of PLECs, interpretation of data, critical review of manuscript drafts and final approval of manuscript for submission.
3. Gunatillake, T – I declare that I participated in and performed some of the thrombin experiments, data analysis and interpretation, critical review and final approval of manuscript for submission.
4. Brennecke, SP – I declare that I participated in the study concept and design, interpretation of data, critical review of manuscript drafts and final approval of manuscript for submission.
5. Ignjatovic, V – I declare that I participated in the study concept and design, performed some of the thrombin experiments, interpretation and analysis of data, critical review of manuscript drafts and final approval of manuscript for submission.
6. Monagle, PT – I declare that I participated in the study concept and design, interpretation of data, critical review of manuscript drafts and final approval of manuscript for submission.
7. Whitelock, JM – I declare that I participated in the study concept and design, interpretation of data, critical review of manuscript drafts and final approval of manuscript for submission.
8. Said, JM – I declare that I participated in the study concept and design, interpretation of data, critical review of manuscript drafts and final approval of manuscript for submission.

Figure 1

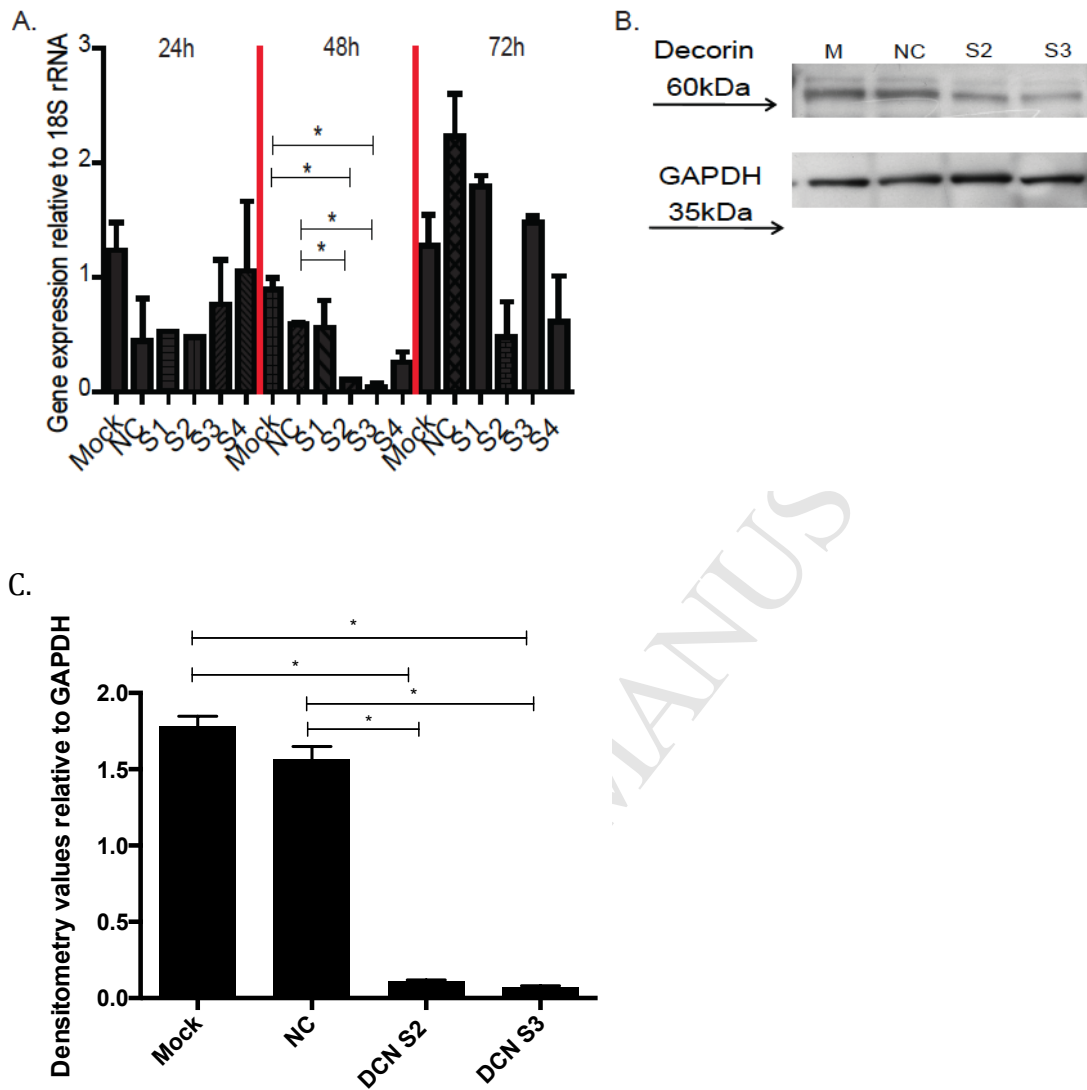


Figure 2

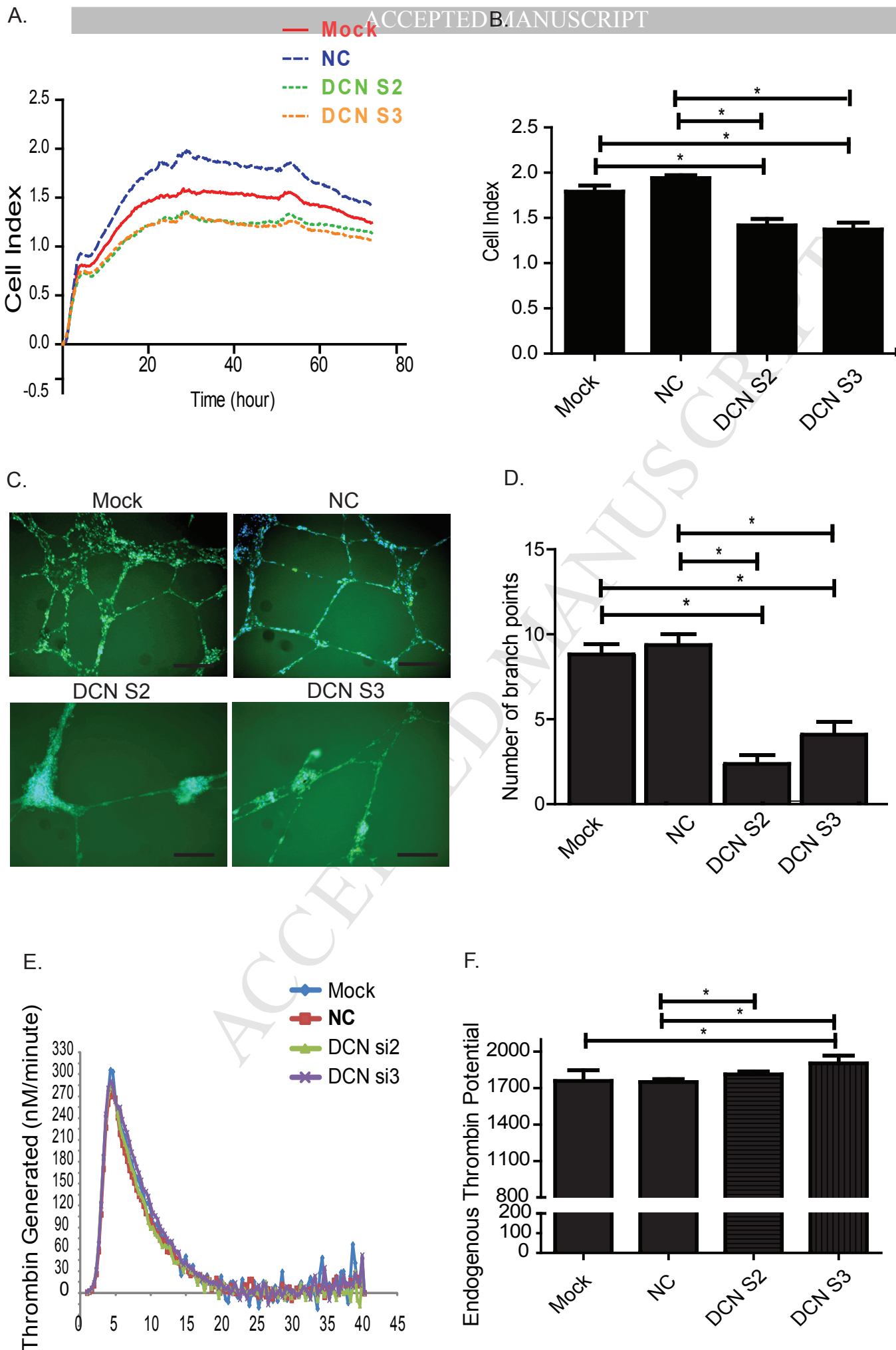


Figure 4

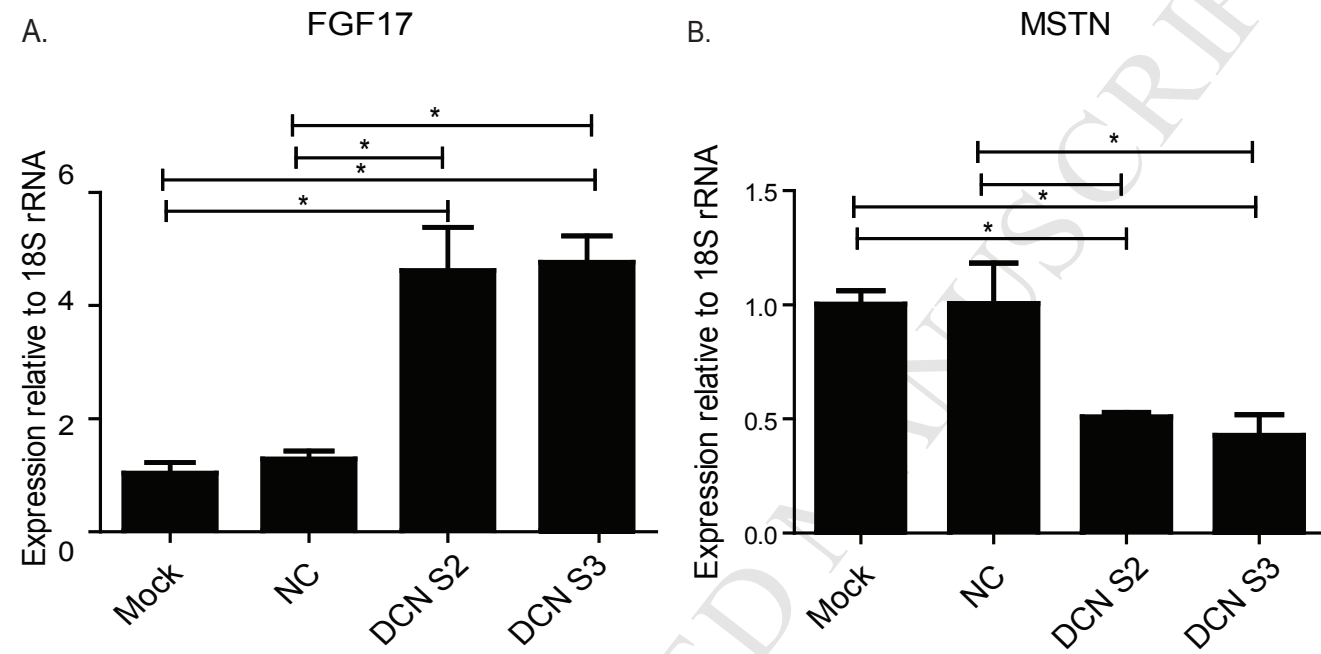


Figure 5

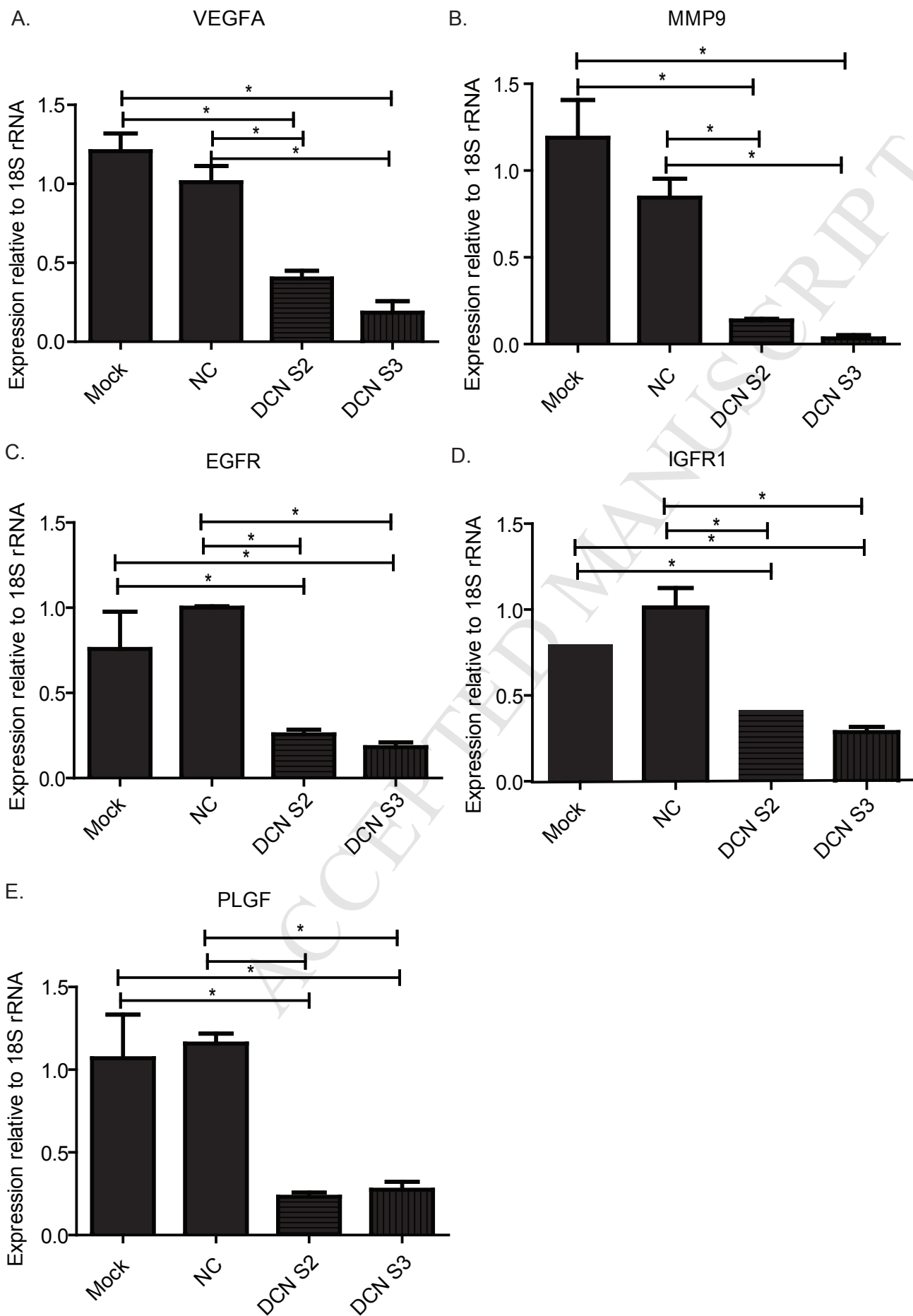
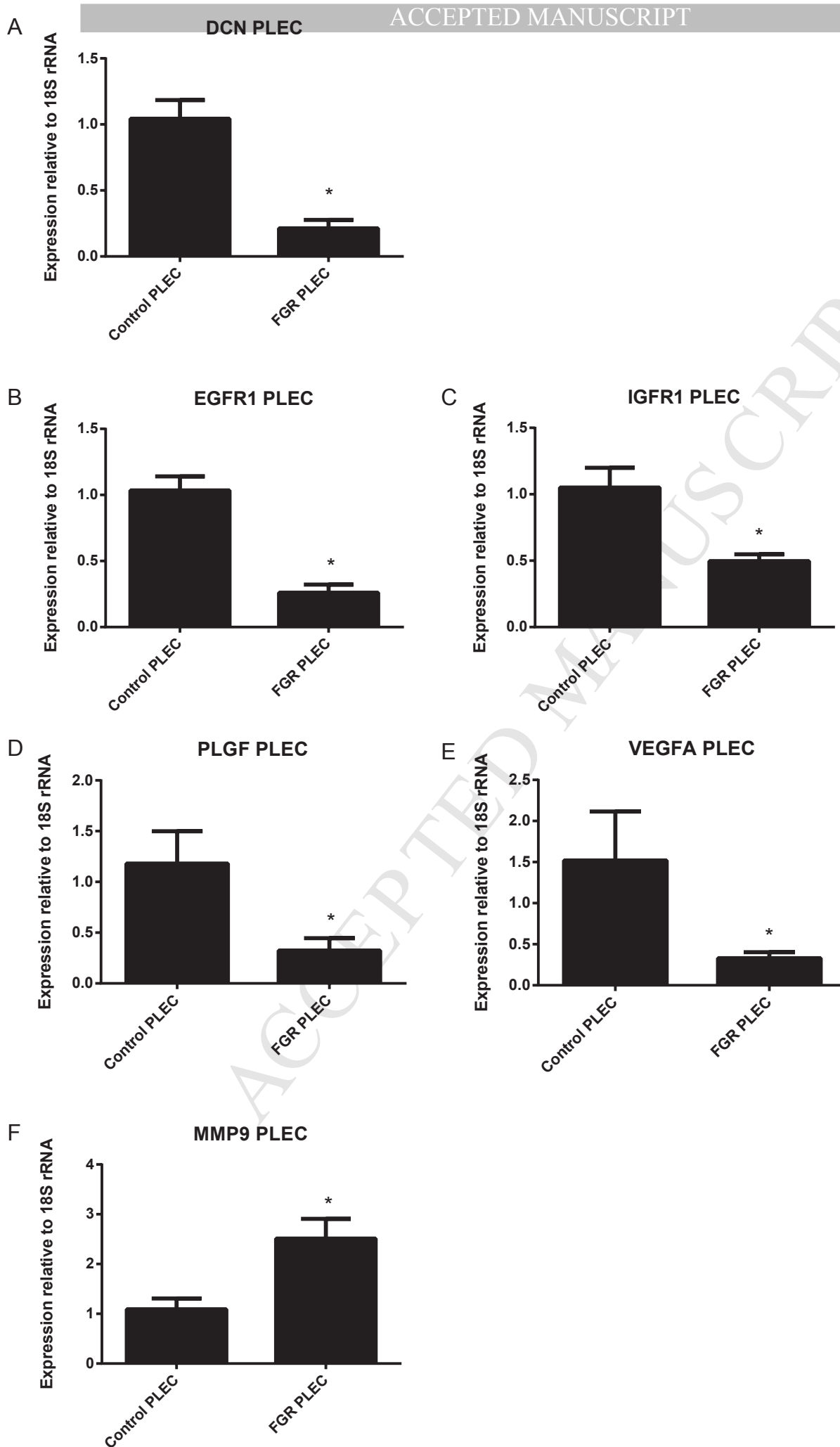


Figure 6



Altered Decorin Leads to Disrupted Endothelial Cell Function: A Possible Mechanism in the Pathogenesis of Fetal Growth Restriction?

Chui A¹, Murthi P^{2,3}, Gunatillake T^{1,3}, Brennecke S.P^{2,3}, Ignjatovic V^{4,5,6}, Monagle P.T^{4,5,6}, Whitelock J.M⁷, and Said J.M¹

Supplementary Data

Materials and methods

Cell lines

The human microvascular endothelial cell line from neonatal foreskin (HMVEC) was a kind gift from A. Prof. Grant Drummond (Department of Pharmacology, Monash University). HMVECs were grown in Microvascular Endothelial Cell Growth Medium-2 (EGM-2 MV Single Quot Kit, catalogue number: CC-4147, Lonza/Clonetics, Victoria, Australia) containing 10% foetal bovine serum (FBS, Murdoch Children's Research Institute Tissue Culture Supplies, Victoria, Australia).

Reduction of DCN expression by siRNA

Four independent *DCN* siRNA oligonucleotides were obtained as "4-For-Silencing siRNA Duplexes"[™] (Qiagen, Victoria, Australia). The *DCN* siRNAs showed no significant DNA sequence similarity to other genes in GenBank cDNA databases (data not shown).

HMVECs were grown in EGM-2 MV and transfected with *DCN* siRNAs using HiPerfect transfection reagent (Qiagen, Victoria, Australia). Negative control (NC) siRNA consisted of a pool of enzyme-generated siRNA oligonucleotides of that were not specific for any known human genes (AllStars Negative siRNA, Qiagen, Victoria, Australia).

RNA extraction and cDNA preparation

Total RNA was extracted from cultured HMVECs using PureLink RNA Mini-kits (Lifesciences, Victoria, Australia), as per manufacturer's instructions. Spectrophotometric analysis was used to determine the yield of total cellular RNA. Total cellular RNA was reverse-transcribed using Superscript III ribonuclease H-reverse transcriptase (Invitrogen, Victoria, Australia) and cDNA was prepared in a two-step reaction using 2µg of total RNA.

Real-Time PCR

Quantification of *DCN* mRNA expression was determined by real-time PCR in an ABI Prism 7700 (Perkin-Elmer-Applied Biosystems, Victoria, Australia) as described previously [1]. Real-time PCR was performed using inventoried assays that consisted of a mix of unlabelled gene-specific PCR primers and TaqMan FAM labelled MGB probes (Applied Biosystems, Victoria, Australia). Gene expression quantification for the housekeeping gene *18S rRNA* MGB endogenous control (Applied Biosystems, Victoria, Australia) was performed in the same well and was calculated according to the $2^{-\Delta\Delta CT}$ method [2].

Western Immunoblotting

Protein was homogenised and extracted from cultured HMVECs using RIPA Buffer (Pierce, Victoria, Australia). Immunoblotting was performed as described elsewhere [1]. An affinity purified rabbit monoclonal antibody for DCN (0.05µg/µl, Abcam, New South Wales, Australia), or rabbit monoclonal GAPDH (1ng/ml Imgenex, South Australia, Australia) was used as the primary antibody. Antibody binding was visualised using peroxidase-conjugated anti-rabbit or IgG-HRP secondary antibody (Dako, Victoria, Australia), following autoradiography using an enhanced chemiluminescence system (Amersham, New South Wales, Australia). The level of immunoreactive DCN protein relative to GAPDH was determined semi-quantitatively using scanning densitometry (Image Quant, New South Wales, Australia).

HMVEC cell growth using xCELLigence

HMVEC cell growth was assessed using the xCELLigence SP real-time system (Roche Diagnostics, Victoria, Australia) according to the manufacturer's instructions. Briefly, cells were prepared and added to the E-Plate 96 (Roche Diagnostics, Victoria, Australia). The xCELLigence system recorded the background electrical impedance for 72h. The results were analysed using the RTCA Software 1.2 (Roche Diagnostics, Victoria, Australia) and GraphPad Prism 5 (GraphPad Software, California, USA).

HMVEC network formation assays

HMVEC network formation was assessed using the µ-Slide Angiogenesis system (IBIDI, Victoria, Australia). Briefly, µ-Slide Angiogenesis wells were coated with 10µl of neat Growth-Factor Reduced Matrigel™ (BD, Victoria, Australia) and allowed to polymerise for 1h at room temperature. HMVECs were then counted and resuspended in treatment media (media ± siRNA) and seeded at a density of 8000 cells in 50µl total volume per well. The slide was returned to the incubator for 48h. The media was then removed, stained with calcein-AM (Millipore, Victoria, Australia) and visualised under a fluorescent microscope. Photomicrographs of entire wells were taken in triplicates and branch points were counted by Wimasis Image Analysis.

Thrombin Generation Assays

HMVECs were plated into 96 well plates at a density of 5000 cells per well and transfected with *DCN* siRNAs and controls for 48h. Venous blood was collected from healthy blood donors (n=40) and Platelet Poor Plasma (PPP) was obtained. Measurement of endogenous thrombin potential (ETP) by Calibrated Automated Thrombogram (CAT, Thrombinoscope, Stago Diagnostica, Victoria, Australia) was performed according to manufacturer's instructions. All experiments were conducted in triplicate wells. The endogenous thrombin potential (ETP) represents the total enzymatic activity performed by thrombin and is generally considered the most predictive parameter of bleeding/thrombosis risk [3, 4]. The ETP (nM/minute) was calculated using the Thrombinoscope software version 3.0.0.29 (Stago Diagnostica, Victoria, Australia) and represents the area under the thrombin generation curve.

Human Growth Factors PCR Array

The "Human Growth Factor" Taqman PCR array (Applied Biosystems, Victoria, Australia) for gene profiling was used to screen for downstream target genes of *DCN*,

according to manufacturer's instructions. The plate contained 84 gene-specific primer sets and a panel of five housekeeping gene primers for normalisation (*18S rRNA*, *B2M*, *HPRT1*, *GAPDH* and *ACTB*). The relative gene expression values, or fold changes, were analysed using DataAssist Software v3.0 (Applied Biosystems, Victoria, Australia) and normalised to the average C_t value of the five housekeeping genes. Candidate genes were prioritised based on level of gene expression i.e. at least 2-fold change in mRNA expression in siRNA treated cells when compared with NC.

References

- [1]. Chui A, Zainuddin N, Rajaraman G, Murthi P, Brennecke SP, Ignjatovic V, et al. Placental syndecan expression is altered in human idiopathic fetal growth restriction. *Am J Pathol.* 2012;180(2):693-702. Epub 2011/12/06.
- [2]. Livak KJ, Schmittgen TD. Analysis of relative gene expression data using real-time quantitative PCR and the 2⁻(Delta Delta C(T)) Method. *Methods.* 2001;25(4):402-8.
- [3]. Castoldi E, Rosing J. Thrombin generation tests. *Thromb Res.* 2011;127 Suppl 3:S21-5. Epub 2011/01/26.
- [4]. Duchemin J, Pan-Petes B, Arnaud B, Blouch MT, Abgrall JF. Influence of coagulation factors and tissue factor concentration on the thrombin generation test in plasma. *Thromb Haemost.* 2008;99(4):767-73. Epub 2008/04/09.



Minerva Access is the Institutional Repository of The University of Melbourne

Author/s:

Chui, A.; Murthi, P.; Gunatillake, T.; Brennecke, S. P.; Ignjatovic, V.; Monagle, P.T.; Whitelock, J. M.; Said, J. M.

Title:

Altered decorin leads to disrupted endothelial cell function: A possible mechanism in the pathogenesis of fetal growth restriction?

Date:

2014-08-27

Publication Status:

Accepted manuscript

Persistent Link:

<http://hdl.handle.net/11343/41988>